Available online at www.sciencedirect.com

SCIENCE DIRECT®

Thin Solid Films 475 (2005) 41–44

thin solid films

www.elsevier.com/locate/tsf

Fabrication of Si nano-pillar array through Ni nano-dot mask using inductively coupled plasma

Mun Ja Kim[a], Jin Seung Lee[b], Seong Kyu Kim[a], G.Y. Yeom[a], Ji-Beom Yoo[a,*], Chong-Yun Park[a]

[a]*Center for Nanotubes and Nanostructured Composite, Sungkyunkwan University, 300, Chunchun-Dong, Jangan-Gu, Suwon, 440-746, South Korea*
[b]*Vacuum and Semiconductor Research Institute, Sungkyunkwan University, 300, Chunchun-Dong, Jangan-Gu, Suwon, 440-746, South Korea*

Available online 9 September 2004

Abstract

We formed Si nano-pillar array using inductively coupled plasma (ICP) etching of Si with Ni nano-dot mask. For the formation of Ni nano-dot mask, Ni was deposited on Si substrate using sputtering. Through rapid thermal annealing (RTA) of Ni layer at 700 °C, Ni nano-dot array was formed on Si substrate. Effects of etching parameters such as rf power, bias voltage and gas composition on the morphologies of Si nano-pillar array were investigated. Optimum etching of Si with Ni nano-dot mask was obtained under the bias voltage of −90 V, power of 1500 W and gas composition of CF_4 (70%) and sulfur hexafluoride (SF_6; 30%). Si nano-pillar array with a diameter smaller than 50 nm and aspect ratio larger than 10 was formed.
© 2004 Elsevier B.V. All rights reserved.

Keywords: Si nano-pillar; Ni nano-dot; Photonic crystal

1. Introduction

Over the past decades, there has been an enormous interest in nanostructure of semiconductors and a lot of progress has been reported [1,2]. A modulation of refractive index of periodic structure results in the appearance of gaps in the electromagnetic spectrum, with characteristics that depend on the dimension of the final system [3]. The photonic nanostructures have been fabricated for one-, two- and three-dimensional photonic bandgap materials [4–8]. Theoretical analysis by Jiang et al. [7] has predicted the presence of quantized confined states in such structures due to the photonic confinement effect, similar to that in semiconductor quantum wells. They showed that the transmission coefficient was united for all the confined states, just like the electronic tunneling in a semiconductor quantum–well system, and the resonant tunneling effect could be used to explain the observed phenomena. Up to now, a periodically arranged structure has been formed by reactive ion etching [9] and electrochemical etching method [10], with an aid of electron beam lithography [11,12]. The photonic crystals of different materials systems formed by various methods have been regarded as key components for the fabrication of various optical wave guides and related devices [13–16].

In this work, we fabricated Si nano-pillar by etching Si substrate using inductively coupled plasma (ICP) etching system with Ni nano-dot array layer. Ni nano-dot array was formed by rapid thermal treatment of Ni layer deposited on Si substrate. Ni nano-dot array layer was used as a mask instead of electron beam (e-beam) lithography. Ni nano-dot mask adopted in this study is not only simple to control but also cheap in the fabrication of uniform nanostructure compared to the conventional lithography technique. Etching characteristics of Si with F-based gases under various conditions were investigated using ICP. Si-nano pillar structure can provide useful routes for electronic devices, data storage and optical devices with enhanced performance and function.

2. Experiments

In order to form the Si-nano pillar array, we performed Si etching using a nanostructured Ni mask. First, we deposited

* Corresponding author. Tel.: +82 31 290 7413; fax: +82 31 290 7410.
E-mail address: jbyoo@yurim.skku.ac.kr (J.-B. Yoo).

0040-6090/$ - see front matter © 2004 Elsevier B.V. All rights reserved.
doi:10.1016/j.tsf.2004.07.026

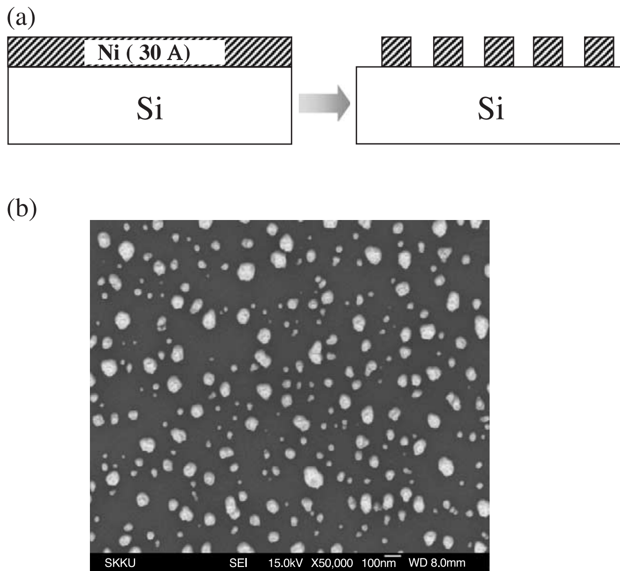

Fig. 1. Formation of Ni nanopatterned mask: (a) schematic diagrams for process of Ni nano-dot formation and (b) field emission scanning electron microscopy (FE-SEM) image of Ni nano-dot formed on Si substrate after RTA at 700 °C.

a very thin Ni layer of 30 Å on Si using sputter system. The Ni deposition rate was 0.3 Å/s at the applied power of 50 W, followed by rapid thermal annealing (RTA) at 700 °C in the N_2 ambient for 10 min. The RTA treatment was carried out at 250 mTorr under the N_2 flow of 30 sccm. We formed the Ni nano-dot pattern on Si substrate.

Using the Ni nano-dot pattern as an etching mask, we performed Si etching using ICP with two radio frequency (rf) sources: one is used for the power generation and the other is used for an ion attraction to the substrate. F-based gases such as sulfur hexafluoride (SF_6) and carbon tetrafluoride (CF_4) were used as an etching gas. We changed rf power from 1000 to 1500 W, and bias voltage from −75 to −90 V.

Effects of etching parameters such as power, bias voltage and gas composition on the Si etching characteristics were investigated and optimized. Si-nano pillar array with diameter smaller than 100 nm was formed. For the analysis of the morphology of Ni nano-dot, etching characteristics and the Si nano-pillar array, field emission scanning electron microscope (FE-SEM: JEOL JSM-6700F) was employed.

3. Results and discussion

We formed Si nano-pillar array using Ni nano-dot array mask by inductively coupled plasma (ICP) etching system. The first step of making Ni nano-dot mask is to deposit Ni thin film on Si substrate using sputtering. The thickness of Ni layer was about 30 Å. We performed rapid thermal annealing (RTA) of Ni thin film at 700 °C for 10 min. Ni thin film deposited on Si substrate was easily conglomerated, resulting in the formation of Ni nano-dot array on Si substrate.

Fig. 1(a) shows the schematic diagram of the procedure for Ni nano-dot array formation using RTA. Fig. 1(b) is FE-SEM image of the Ni nano pattern formed on Si substrate. The average diameter of Ni nano-dot is 60±15 nm. The thin film deposition and RTA process is not only an easy and simple technique to control the formation of nano-dot but also a cost-effective process compared to the conventional nano-pattern formation process like electron beam lithography technique. The size and distribution of the nano-dots on the Si substrate were mainly determined by thin film thickness the RTA temperature. The diameter of nano-dots became smaller with a decrease in the thickness of deposited Ni layer.

We investigated the effect of etching power on the etching characteristics of Si. We carried out Si etching using SF_6 with Ni nano-dot mask under the following conditions: bias voltage of −100 V, chamber pressure of 10 mTorr and etching time of 2 min. As shown in Fig. 2(a), inhomogeneous particles of by-products were formed and the formation of nano-pillar was hardly observed at the power of 1000 W. But as the power increases up to 1500 W, a little improvement in the formation of nano-pillar was observed with decrease in a formation of inhomogeneous particles. (Fig. 2(b)) Because the increase in etching power enhanced the etching rate of Si, Si nano-pillar formation became feasible. However, in the case of etching of Si with SF_6 gas, etching selectivity between Ni nano-dot mask and Si was generally poor, irrespective of the applied power, resulting in the failure of the formation of Si nano-pillar.

We studied the effect of bias voltage and gas composition on morphologies of Si-nano pillar. We changed the bias voltage from −75 to −90 V. To prevent the formation of by-product from etching as well as to improve the etching

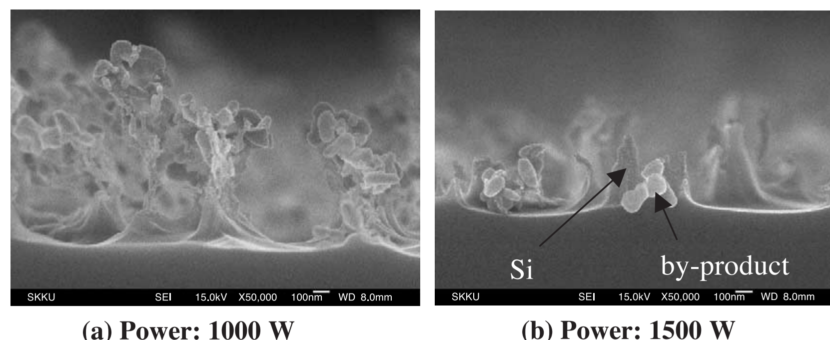

Fig. 2. FE-SEM images of morphology of Si substrate after etching with different RF power: (a) 1000 to (b) 1500 W.

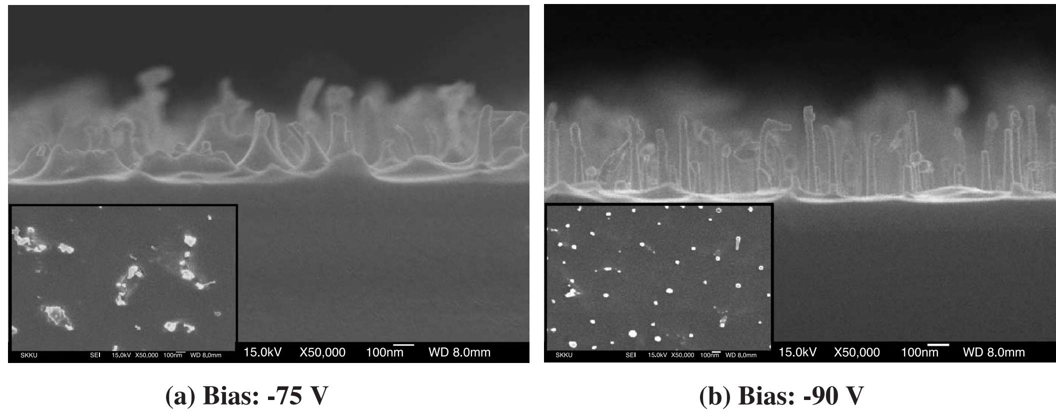

Fig. 3. FE-SEM images of Si-nano pillar array formed under the bias voltage: (a) −75 to (b) −90 V. Inset is top view.

selectivity between Ni nano-dot mask and Si, we added CF_4 to SF_6. The ratio of flow rate of SF_6 to CF_4 was 30 to 70. The Si was etched under the etching power of 1500 W. As shown in Fig. 3, with an addition of CF_4 to SF_6, etching selectivity between Si and Ni was improved and formation of by-product was drastically reduced. Fig. 3(a) and (b) showed that the increase in bias voltage from −75 to −90V results in the formation of sharp nano-pillar, with high aspect ratio of 12 and clean surface. Insets of Fig. 3(a) and (b) show the top view of SEM image of Si-nano pillars

Fig. 4. FE-SEM images of Si-nano pillar array formed under different gas composition: (a) SF_6, (b) SF_6(90)+CF_4(10), (c) SF_6(50)+CF_4(50), (d-1) tilt-view of SF_6(30)+CF_4(70), (d-2) cross-sectional view of SF_6(30)+CF_4(70), (e) SF_6(10)+CF_4(90), and (f) CF_4(100).

formed by ICP etching. As the bias voltage increases from −75 to −90 V, separation between Si nano-pillars was obtained, resulting in the isolation of each Si nano-pillar. The diameter and height of the formed Si nano-pillar is about 41 and 472 nm, respectively.

We systematically investigated the effect of gas composition on the etching characteristics of Si for the formation of nano-pillar array. The experiments with different gas composition were conducted under the following conditions: rf power was 1500 W, bias voltage was −90 V, the process pressure was 10 mTorr and etching time was 2 min. As the CF_4 content in etching gas increases up to 90% (see Fig. 4 from (a) to (f)), morphologies of the Si nano-pillar changed drastically. The change in the density of Si nano-pillar was also observed with variation of gas composition as shown in Fig. 4. Comparison of Fig. 4(a) with Fig. 4(f), etching selectivity between Ni nano-dot mask and Si is better in the etching with CF_4 than SF_6. However, the etching rate of Si with SF_6 is faster than that of Si with CF_4. As the content of CF_4 increases up to 50%, etching selectivity improved, but the overall etching characteristics was still dominated by SF_6. As shown in Fig. 4(c), Si under the small Ni nano-dot was completely etched away; only Si masked by relatively large Ni nano-dot remains after etching, resulting in the very low density of Si nano-pillar. At the composition of CF_4 (70%) and SF_6 (30%), etching selectivity between Si and Ni mask came to play an important role in Si nano-pillar formation. Etching selectivity was balanced with etching rate. As the CF_4 content increases further, etching selectivity increases while the etching rate decreases, leading to the formation of highly dense Si nano pillar array (Fig. 4(e), (f)). As shown in the tilt view of SEM image (Fig. 4(d-1)), Si nano-pillar array clearly forms: the interdistance and the height of Si nano-pillar is about 220 and 470 nm, respectively. The average diameter of nano-pillar is about 40 nm which is smaller than that of Ni nano-dots used as a mask layer. For Si etching, the fluorine is an active etchant, and etch rate was determined by the fluorine content. From these results in Fig. 4, the optimum gas composition for the Si pillar array formation, with an aspect ratio higher than 10, was SF_6 (30%) and CF_4 (70%).

4. Summary

We fabricated the Si nano-pillar array using inductively coupled etching with Ni nano-dot mask. Ni nano-dot pattern on Si substrate was formed by deposition of Ni thin layer of 30 Å, followed by RTA process at 700 °C. Using this Ni nano-dot mask, we carried out Si etching experiments using ICP system. We investigated the Si etching characteristics as a function of rf power, bias voltage and gas composition. As the rf power increased from 1000 to 1500 W, formation of by-product decreased and formation of Si nano-pillar slightly improved. As the bias voltage increased from −75 to −100 V, formation of Si nano-pillar with clean sidewall improved. As CF_4 composition in etching gas increased, etching selectivity enhanced. We got the Si nano-pillar array with aspect ratio higher than 10 at the etching gas composition of SF_6 (30%) and CF_4 (70%).

Acknowledgements

This work was supported by KOSEF through CNNC.

References

[1] L. Esaki, R. Tus, IBM J. Res. Develop. 14 (1970) 61.
[2] E.E. Mendez, K. von Klitzing (Eds.), Physics and Application of Quantum Wells and Superlattices, Plenum, New York, 1987, pp. 261–376.
[3] See for example, J.D. Joannoploulos, R.D. Meade, J.N. Winn (Eds.), Photonic Crystals, 'Molding the Flow of Light', Princeton Univ. Press, Princeton, NJ, 1995, pp. 38–93.
[4] (a) S.Y. Lin, G. Arjavalingam, J. Opt. Soc. Am. B 11 (1994) 2124;
(b) S.Y. Lin, G. Arjavalingam, Opt. Lett. 18 (1993) 1666;
(c) S.Y. Lin, V.M. Hietala, S.K. Lyo, A. Zaslavsky, Appl. Phys. Lett. 68 (1996) 3233.
[5] J. Zi, J. Wan, C. Zhang, Appl. Phys. Lett 73 (1998) 2084.
[6] F. Qiao, C. Zhang, J. Wang, J. Zi, Appl. Phys. Lett. 77 (2000) 3698.
[7] Y. Jiang, C. Niu, D.L. Liu, Phys. Rev., B 59 (1999) 9981.
[8] S. Yano, Y. Segawa, J.S. Bae, K. Mizuno, H. Miyazaki, K. Ohtaka, S. Yamaguchi, Phys. Rev., B 63 (2001) 153–316.
[9] D. Crouse, A. Yu-Hwa Lo, E. Miller, M. Crouse, Appl. Phys. Lett. 76 (2000) 49.
[10] S.H. Xu, Z.H. Xiong, L.L. Gu, Y. Liu, X.M. Ding, J. Zi, X.Y. Hou, Appl. Phys., A 76 (2003) 589.
[11] D. Peyrade, Y. Chen, A. Talneau, M. Patrini, M. Galli, F. Marabelli, M. Agio, L.C. Andreani, E. Silberstein, P. Lalanne, Microelectron. Eng. 61–62 (2002) 529.
[12] M. Francois, J. Danlot, B. Grimbert, P. Mounaix, M. Muller, O. Vanbesien, D. Lippens, Microelectron. Eng. 61-62 (2002) 537.
[13] S. Fan, R. Villeneuve, J.D. Joannopoulos, H.A. Hauss, Phys. Rev. Lett. 80 (1998) 960.
[14] E. Yablonovitch, T.J. Gmitter, K.M. Leung, Phys. Rev. Lett. 67 (1991) 2295.
[15] P. Pottier, et al., J. Lightwave Technol. 17 (1999) 2058.
[16] D.D. Labilloy, H. Benisty, C. Weisbuch, Appl. Phys. Lett. 71 (1997) 738.